View Article Online
DOI: 10.1039/C9NR04202D

Solvothermal Synthesis of Graphene Oxide and its Composites with Poly(ε-caprolactone)

*Seow Jecg Chin[1], Matthew Doherty[2], Sesha Vempati[2], Paul Dawson[2], Cormac Byrne[3], Brian J. Meenan[3], Valentina Guerra[4] and Tony McNally[4]**

[1]School of Mechanical and Aerospace Engineering, and [2]Centre for Nanostructured Media, School of Mathematics and Physics, Queen's University Belfast, BT9 5AH, UK.

[3]Nanotechnology & Integrated Bioengineering Centre (NIBEC), School of Engineering, Ulster University, BT37 0QB, UK.

[4]International Institute for Nanocomposite Manufacturing (IINM), WMG, University of Warwick,, CV4 7AL, UK.

*Corresponding author E-mail: t.mcnally@warwick.ac.uk

View Article Online
DOI: 10.1039/C9NR04202D

Abstract

Graphene oxide (GO) was prepared by a solvothermal synthesis method using sodium and ethanol. A sequence of pyrolysis, washing and purification steps was developed for the total removal of all by-products. The first pyrolysis step is essential to obtain graphitic forms of carbon while a washing and a second pyrolysis step further improved the graphenic structures obtained via the reduction of OH/COOH and C-O groups and the attendant increase in C=C bonding (sp^2 hybridization). Two purification processes were employed to remove sodium carbonate (by-product), i.e. vacuum filtration and centrifugation, but the latter produced a more stable GO product, typically with a few-layer (*ca* 3nm) stack and relatively long platelets (up to *ca* 1.3 μm). The functionality of this GO was demonstrated by preparing composites of it with poly(ε-caprolactone) (PCL). The GO was arranged in flower-like domains dispersed in the PCL matrix. The crystalline content of PCL decreased on addition of GO, though the dynamic modulus of PCL increased and an electrical percolation at 0.5vol% GO was obtained, manifest by a ~10^4 increase in electrical conductivity (in an overall increase of ~10^5 achieved at > 1vol%), more than sufficient for anti-static applications.

1. Introduction

GO is a promising material for use as a functional additive in polymer systems with applications as diverse as in engineering composites, transistors, sensors and biomedical devices [1-3].

GO was first discovered by B. C. Brodie in 1859 who synthesized it by the chemical reaction of potassium chlorate ($KClO_3$) and a slurry of graphite in fuming nitric acid

View Article Online
DOI: 10.1039/C9NR04202D

(HNO_3). Since then, other routes have been developed to synthesize GO, all mostly involving chemical reaction in harsh environments, such as in the Staudenmaier method (1898), Hummers method (1958) and the modified Hummers' method (1999-2004). The procedures realized by Brodie and Staudenmaier generates ClO_2 gas, which is toxic and explosive in an air atmosphere. Moreover, the reaction time is quite long, ranging from 1 to 5 days. The modified Hummers' method does not evolve any toxic substance but the residual excess of permanganate ions from the potassium permanganate ($KMnO_4$) used during the reaction is a limitation since it decreases the quality of the final material [4, 5].

An innovative route to synthetize GO is offered by solvothermal reactions. To the best of our knowledge, only a few papers have been published describing the solvothermal process as an alternative route to prepare GO and other graphenic forms of carbon [6-16]. There are a number of benefits of the solvothermal approach for producing GO: i) it is cost-effective, nontoxic and, uses a minimum number of common laboratory reagents, and ii) the reaction can proceed with almost no byproducts. The synthesis procedure described herein entails 4 steps: precursor synthesis, 1st pyrolysis, washing and 2nd pyrolysis [6], followed by a final purification step. This approach results in the production of high quality GO with a structure closer to the pure graphenic form, which is known to present better mechanical, thermal and electrical properties [17, 18].

The use of GO in poly(ε-caprolactone) (PCL), especially for reinforcement and control of electrical conductivity in the resulting composite materials, has not been investigated in detail [19-25]. Herein, we also demonstrate the usefulness of the solvothermal synthesized GO as an additive to PCL to prepare composite materials with a

View Article Online
DOI: 10.1039/C9NR04202D

high storage modulus (up to *ca* 260 MPa) and low electrical percolation threshold (0.5 vol% GO).

2. Experimental

2.1. Synthesis of Graphene Oxide (GO)

Step 1: sodium, 2g (Sigma Aldrich 13401, ≥99% purity) and ethanol, 5ml (T.E. Laboratories Ltd, IMS 94) in the molar ratio 1:1, were added in turn to a sealed vessel (Parr Intrument Company 4744) and transferred to a heating oven for solvothermal reaction at 220 °C for 72h.

Step 2: the reaction product, white with a brownish tinge, was then subjected to pyrolysis until it turned greyish-black in colour.

Satep 3: after washing with deionised water and subsequent vacuum filtration, the graphene/GO was dried in a vacuum oven for at least 24h to remove residual water. The as-produced graphene/GO appeared now as a fluffy, porous material. The yield of the graphene/GO was typically around 0.5g and the process was repeated until adequate quantities were obtained for melt mixing with PCL.

Step 4: in an attempt to remove residual functional groups, the graphene/GO product, was washed and pyrolysed for 3 mins at a maximum attainable temperature of 2000 °C. In the context of this work, the material is henceforth referred to as GO.

2.2. Purification of Graphene Oxide (GO) Products

The final step (5) in the solvothermal process adopted in this work was purification. Two methods were employed to remove the remaining sodium carbonate (Na_2CO_3) impurities

View Article Online
DOI: 10.1039/C9NR04202D

from the as-produced GO. Firstly, the product was diluted with 22g/100ml deionised water and placed in a centrifuge tube, followed by vigorous shaking to give a brown dispersion prior to centrifugation (IEC CL10, DJB Labcare) at 4000 rpm for one hour. The top 85% of supernatant was pipeted off and the sediment centrifuged again in fresh deionised water. The centrifuge purification process was repeated until the pH level of supernatant became constant at pH 7. The sediment was then collected, air-dried and placed in an oven at 100 °C for 24h to eliminate residual water. The second method, involved preparing a solution of 22g/100ml of as-produced GO in deionised water in a beaker which was then mechanically agitated until homogenization was achieved using a magnetic stirrer (HB502, Bibby) at ambient temperature. The GO was collected by filtration and dried in an oven at 100 °C for 24h. The purity of the GO that resulted from each of the purification methods was investigated using a range of characterisation techniques, including TGA, four-point probe method, Raman spectroscopy, XPS, FTIR and FESEM-EDX.

2.3. Characterisation of Graphene Oxide (GO) Products

The Raman spectra of HOPG (as a fingerprint), graphene precursor (i.e. prior to pyrolysis) and solvothermal synthesised GO was collected on a custom-built, open bench Raman system in the backscattering configuration with a laser excitation of wavelength 532 nm. To quantitatively analyse the surface chemistry of the graphene, X-ray photoelectron spectroscopy (XPS) was carried using a Kratos Axis Ultra DLD spectrometer (Kratos, UK) using monochromated AlKα X-ray (1486.6 eV) radiation. Wide energy survey scans and high resolution spectra were obtained at pass energies of

View Article Online
DOI: 10.1039/C9NR04202D

160eV and 20eV, respectively. All binding energy values were charge compensated by assigning the main C1s peak at 284.5eV to the presence of a graphitic component with 100% sp^2 bonding [39]. Spectra were recorded with the high vacuum analysis chamber of the instrument operating at a pressure of less than 5 x 10^{-8} mbar. The resulting quantitative data were obtianed using the associated Kratos data processing software. The dried GO powder and pyrolysed product were also characterised by Fourier transform infrared spectroscopy (FTIR, PerkinElmer Spectrum 100 spectrometer) using KBr discs. The spectra were recorded in transmission mode using Spectrum 6.3.4.0164 software by co-adding 64 scans in the spectral range 450cm^{-1} to 4000cm^{-1} with 4cm^{-1} resolution. Field Emission Scanning Electron Microscopy (FESEM) images of GO were obtained using a JEOL JSM-6500F FESEM instrument. Prior to examination using High Resolution Transmission Electron Microscopy (HRTEM) GO was deposited on holey carbon-coated 300 mesh copper grids and images collected with a FEI (previously Philips Electron Optics) Tecnai F20 transmission electron microscope operating at 200kV. After depositing the GO onto a gold substrate, thickness measurements were made by Atomic Force Microscopy (AFM), using a Digital instruments Nanoscope IIIa, operating in tapping mode with subsequent analysis carried out using NanoScope6.12r1 software. Wide-angle X-ray diffraction (WAXD) spectra were obtained using a PANalytical's X'Pert Pro Multi-Purpose Diffractometer (MPD) using Cu-K_α radiation of wavelength 1.5418367Å at a scan rate of 0.02 2Θ/min. The KBr pellet device used for the FTIR sample preparation was also used to prepare pellets of pressed GO for electrical conductivity measurements by a four-point method (probe spacing: 3.54mm) using a Keithley 6221 AC/DC current source combined with a Agilent 34401A Multimeter. The

View Article Online
DOI: 10.1039/C9NR04202D

thermal stability of GO was measured using a Mettler-Toledo TGA/SDTA851e/LF/1600°C in the temperature range 25 °C to 1200 °C with a heating rate of 10 °C /min in nitrogen.

2.4 Preparation and Characterisation of Composites of PCL and GO

CAPA 6506 PCL, in powder form, with an average molecular weight of 50,000 and density of 1.1g/cm^3 was supplied by Perstorp, UK (formerly Solvay, Belgium). GO was ground into a fine powder using a mortar and pestle and premixed with the PCL in a Rondol Technology high speed mixer, model DAC 150FVZ. The mixer was centrifugally rotated for 30s at 2400 rpm for each dry blend. Composites of PCL and GO at loadings up to 7wt% were made by melt mixing using a Thermo Scientific HAAKE Rheomex PTW16 OS mini twin screw compounder at 70 °C to 85 °C with a screw speed of 120 rpm. Dynamic Mechanical Analysis (DMA) was performed on the composite materials using a Polymer Laboratories Thermal Sciences 190-19 Dynamic Mechanical Thermal Analyzer, operated in dual cantilever mode from -120 °C to 50 °C at 1Hz, with a constant strain of x4 and a heating rate of 2 °C/min. Differential scanning calorimetry (DSC) analysis was performed using a Perkin Elmer Diamond DSC using a heating and cooling rate of 10 °C/min. from -20 °C to 100 °C. Thermogravimetric analysis (TGA) of all composites was carried out in the temperature range 25 °C to 500 °C at a heating rate of 10 °C/min. The direct current (DC) electrical resistivity of PCL and PCL/GO composites was measured in compliance with ASTM D257-07 using a Keithley model 6517A electrometer. The macroscale dispersion of the graphene in PCL was also investigated using optical microscopy (OM), (Nikon Eclipse ME600 microscope). Extruded strands of

View Article Online
DOI: 10.1039/C9NR04202D

the composites were microtomed to an approximate thickness of 10μm, placed on a hot stage and melted at 60 °C. Extruded strands were also cryo-fractured and sputter coated with gold prior to examination in the FESEM. WAXD patterns of composites were obtained, using the same FESEM instrument described above, to determine the effect of the GO addition on the crystalline content of PCL.

3. Results and discussion

3.1 GO characterization

As indicated, the first step in the solvothermal process is the reaction between sodium and ethanol at 220°C for 72h, which leads to the synthesis of the precursor for GO. The possible reactions involved during this phase of the process are:

- Ethanol + Sodium → Sodium Ethoxide + Hydrogen [26] (1)

  $2C_2H_5OH + 2Na \rightarrow 2C_2H_5ONa + H_2$

- Sodium Ethoxide + Water → Sodium Hydroxide + Ethanol [26] (2)

  $C_2H_5ONa + H_2O \rightarrow NaOH + C_2H_5OH$

- Sodium Hydroxide + Carbon Dioxide → Sodium Carbonate + Water [26] (3)

  $2NaOH + CO_2 \rightarrow Na_2CO_3 + H_2O$

  Or (depending on the reaction propotions)

  Sodium Hydroxide + Carbon Dioxide → Sodium Bicarbonate [26]

  $NaOH + CO_2 \rightarrow NaHCO_3$

- Sodium Carbonate + Carbon Dioxide + Water → Sodium Bicarbonate [26] (4)

  $Na_2CO_3 + CO_2 + H_2O \rightarrow 2NaHCO_3$

View Article Online
DOI: 10.1039/C9NR04202D

No graphitic form of carbon is produced during this phase of the solvothermal synthesis as confirmed by Raman spectroscopy in that Figure 1(a) proves the absence of G and D bands typical of graphite and its derivatives. Pyrolisis (second phase) does produce graphitic forms of carbon as evident from the Raman spectra shown in Figure 1(b) of the (pyrolized) product:

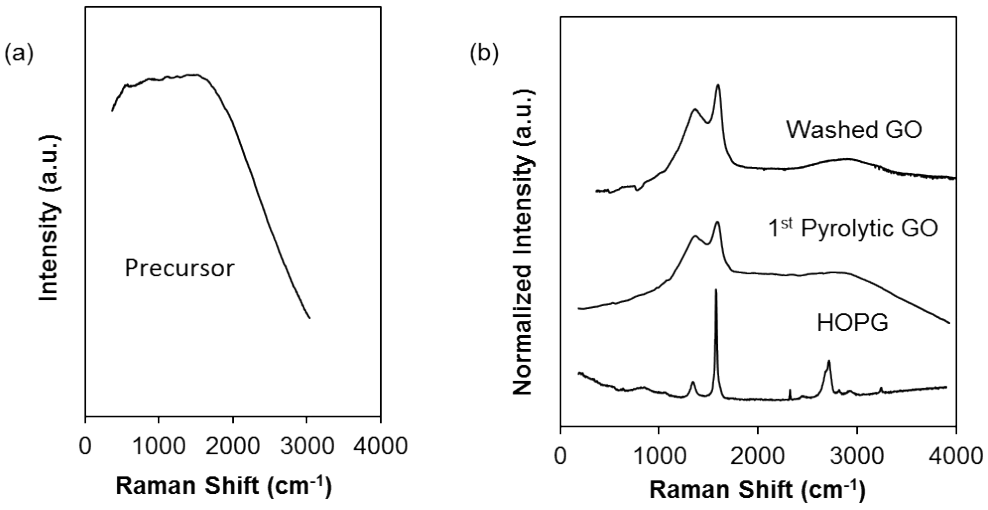

Figure 1: Raman spectra of GO precursor (a). Comparison of Raman spectra for HOPG, 1st stage pyrolysed GO and washed (pyrolysed) GO (b).

The 1st step in the solvothermal process has clearly produced pyrolytic GO as proved by the presence of the D band at *ca* 1350 cm^{-1} and G band at *ca* 1580 cm^{-1} in Raman plot 1(b) [27, 28]. The spectrum for High Ordered Pyrolytic Graphite (HOPG) is also reported as reference to identify the typical expected graphitic peaks [29]. Washing the pyrolized product, increases the quality of GO crystallites (in terms of a reduction in the concentration of defect sites) as evident from the increase in the intensity of the G‘ band from the pyrolized GO to the washed product [27, 28].

View Article Online
DOI: 10.1039/C9NR04202D

XPS analysis was performed to determine the chemical composition at the surface of the pyrolized and washed products. The relative quantitative contributions of the elemental species detected for the 1st stage pyrolized and subsequently washed products are illustrated in Figure 2 (a) and (c). The contributions to the devonvolued C1s spectra for each material are provided in Figure 2 (b) and (d).

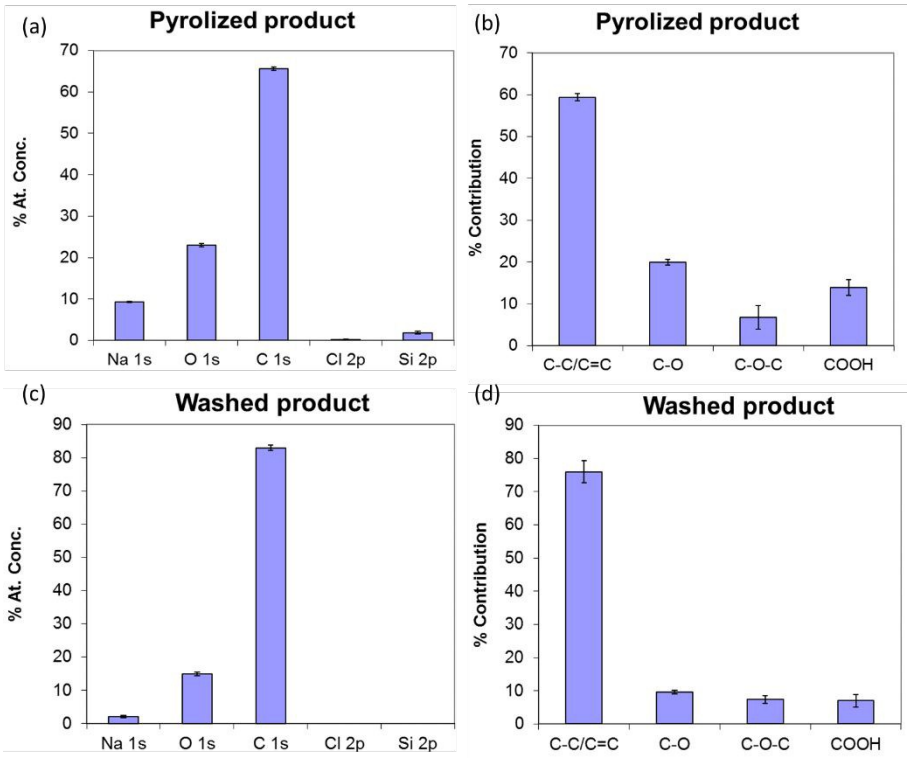

Figure 2. XPS elemental quantitative data, reported as the percentage atomic concentration (%At. Conc.) for each species detected for 1st stage pyrolyzed product (a) and washed product (c). Contributions to the deconvoluted C1s spectral region are shown for the pyrolyzed product (b) and washed product (d).

The main atomic species detected by XPS analysis for the pyrolized (a) and washed (c) products were Carbon (C1s), Oxygen (O1s) and Sodium (Na1s). The chemical species contributing to the C1s spectral region was determined to be C-C/C=C, C-O, COOH, C-

View Article Online
DOI: 10.1039/C9NR04202D

O-C for both materials (b,d)[4, 27]. At the elemental level, the washing phase resulted in an increase in the carbon content from *ca* 65 %At. Conc. to *ca* 83 %At. Conc. and a reduction in the oxygen content from *ca* 22 %At. Conc.to *ca* 12 %At. Conc. These data suggest that after washing the product shows a reduction in the number of oxidized sites. Consideration of the C1s region confirms a significant decrease in C-O groups (from 20% to 10%) and COOH groups (from 13% to 8%) contribution to the spectral envelop with the concurrent increase in the C-C/C=C bond percentage (from 60% to 75%). This translates to a material with a structure closer to the graphenic form of carbon, having less (dangling) oxidized bonds and thus is of higher crystalline quality. As such, the findings from XPS are in agreement with interpretation of the Raman spectra.

The second pyrolysis step that is performed in the solvothermal process (fourth phase) was adopted to further improve the quality of the graphenic structure in the final product. It is therefore expected that a further reduction of C=O bonds in favour of the C-C=C arrangement in typical graphenic aromatic structures should result. To investigate this effect, FTIR was performed on both the first and second pyrolised products, as shown in Figure 3.

View Article Online
DOI: 10.1039/C9NR04202D

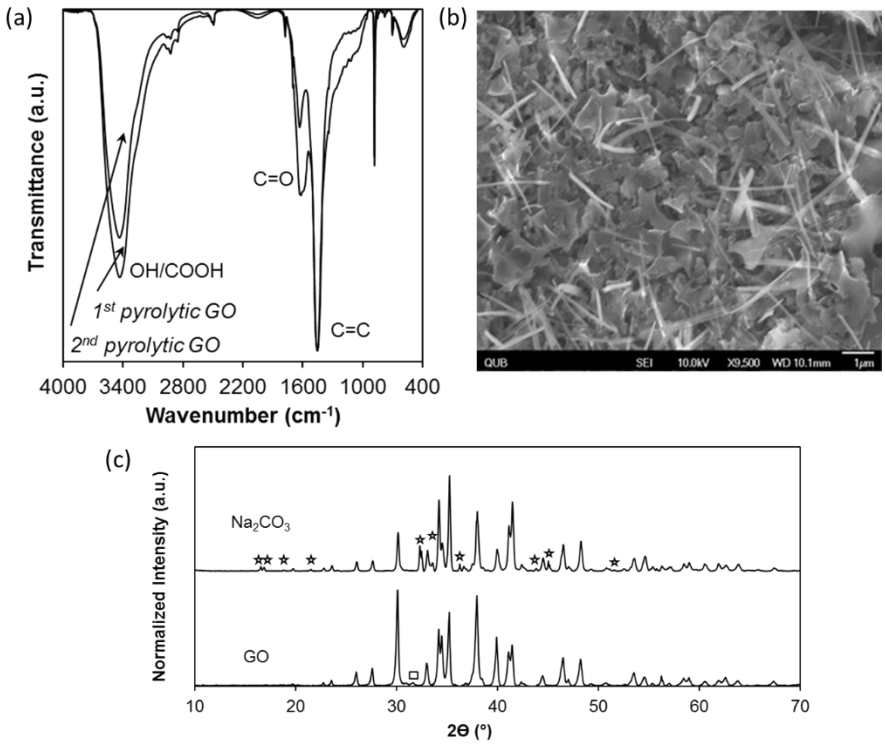

Figure 3. a) FTIR of 1st and 2nd pyrolyzed GO product, b) FESEM image of GO with sodium carbonate rod-like shape impurities and c) wide angle XRD plots of purified GO and sodium carbonate (as reference).

The reduction in the intensity of both the OH/COOH peak at 3400cm^{-1} and the C=O peak at 1700cm^{-1} along with the increase of the C=C peak at 1600cm^{-1} in the second pyrolitic product (Figure 3(a)) confirms the expected increase in carbon-carbon bond content and the reduction of oxidized sites after the second pyrolysis [30]. Hence, the GO product after the second pyrolysis has only a minor concentration of oxide and hydroxide groups, such that a more graphenic structure is obtained.

The FESEM image of the product obtained after the second pyrolisis step (Figure 3(b)) shows the presence of GO platelets along with a rod-like shape material which has been

View Article Online
DOI: 10.1039/C9NR04202D

ascribed to the presence of sodium carbonate that is produced during the solvothermal reaction as main by-product.

In order to further study the presence of sodium carbonate, XRD analysys was performed with the diffractograms shown in Figure 3(c). The typical XRD spectrum of graphene presents a peak at $2\theta=26^{o}$ due to the (002) crystallographic plane. This peak is shifted at $2\theta=10^{o}$ in GO spectra [31]. However, in the XRD spectra obatined it is not easy to identify this peak due to the overlapping of the peaks of sodium carbonate. However, the presence of sodium carbonate impurity is confirmed.

Purification procedures (fifth phase) were adopted to remove the by-product impurities. As explained in the experimental section, two types of purification pocess were performed, namely centrigugation and vacuum filtration. The materials obtained from each procedure were analysed by TGA/DTGA and the results are reported in Figure 4.

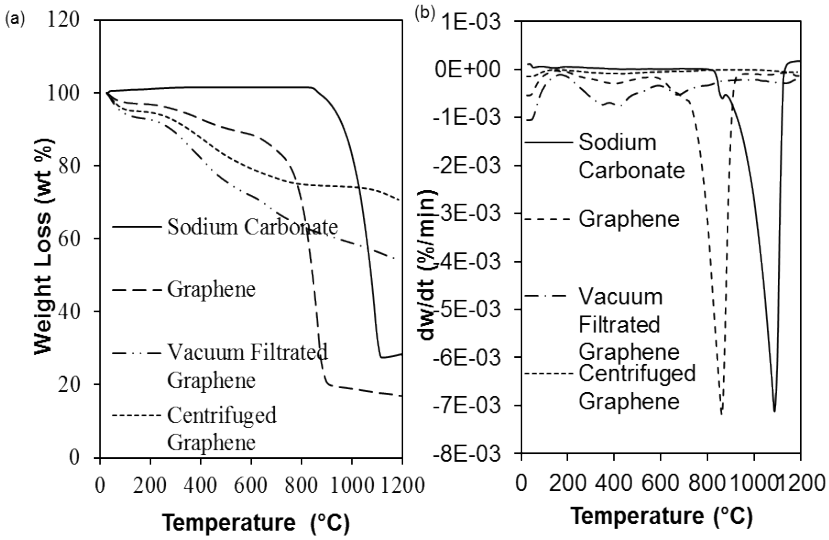

View Article Online
DOI: 10.1039/C9NR04202D

Figure 4: TGA (a) and DTGA (b) thermograms of GO (reference), sodium carbonate and GO as synthesized here, after separate purification by vacuum filtration and centrifugation.

It is evident that a reduction in the thermal stability of the GO product occurs on removal of the sodium carbonate by-product using both purification procedures. However, the data suggest that the centrifuged product is the more stable of the two, with a weight loss of *ca* 5% at 100ºC, which may be due to removal of residual physically adsorbed water and a further weight loss of *ca* 25% at 450 ºC associated with weakly bound oxygen functional groups

FESEM-EDX experiments were performed on the centrifuged GO product to prove the efficiency of the purification step adopted by detecting the presence, if any, of sodium carbonate, see Figure 5.

View Article Online
DOI: 10.1039/C9NR04202D

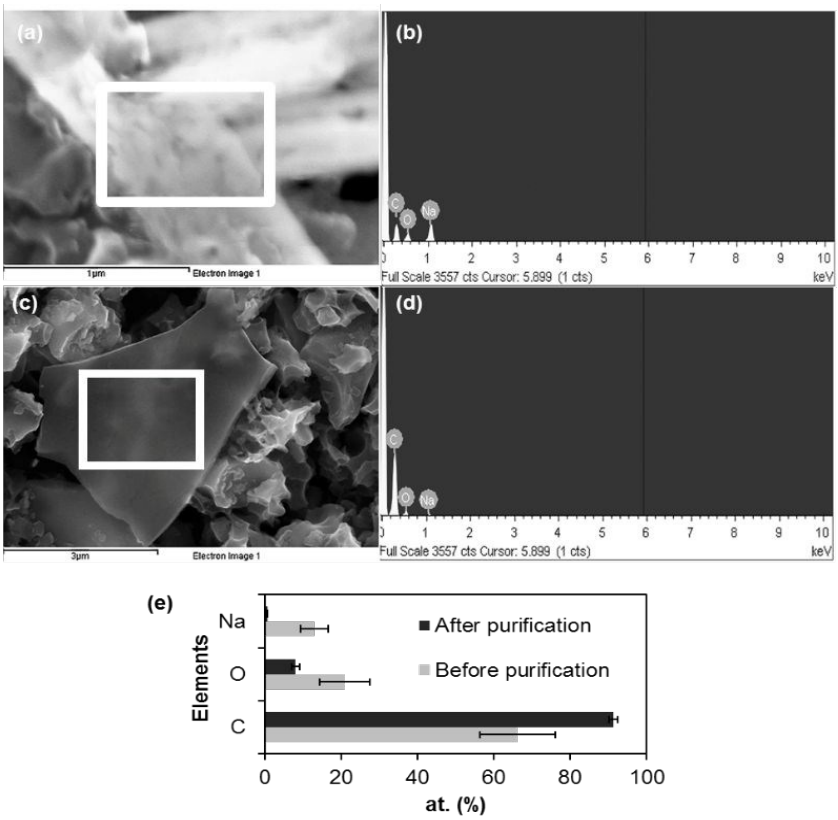

Figure 5. FESEM images of GO before and after purification by centrifugation (a,c) and related EDX spectra (b,d). Bar chart shows the atomic composition (weight percentage) of each element before and after centrifugation (e).

It is clear from the EDX data that there is a significant reduction of both oxygen and sodium from *ca* 20% and *ca* 17% to *ca* 10% and *ca* 1%, respectively, suggesting the almost complete by-product removal. The increase in the percentage of carbon may be ascribed to the uptake of CO_2 during the air-drying phase which can be trapped between GO sheets. If this hypothesis is correct, it would imply that the final oxygen content is even lower than the 10% detected.

The centrifuged GO was further analysed by FESEM, TEM and AFM, as shown in Figure 6.

View Article Online
DOI: 10.1039/C9NR04202D

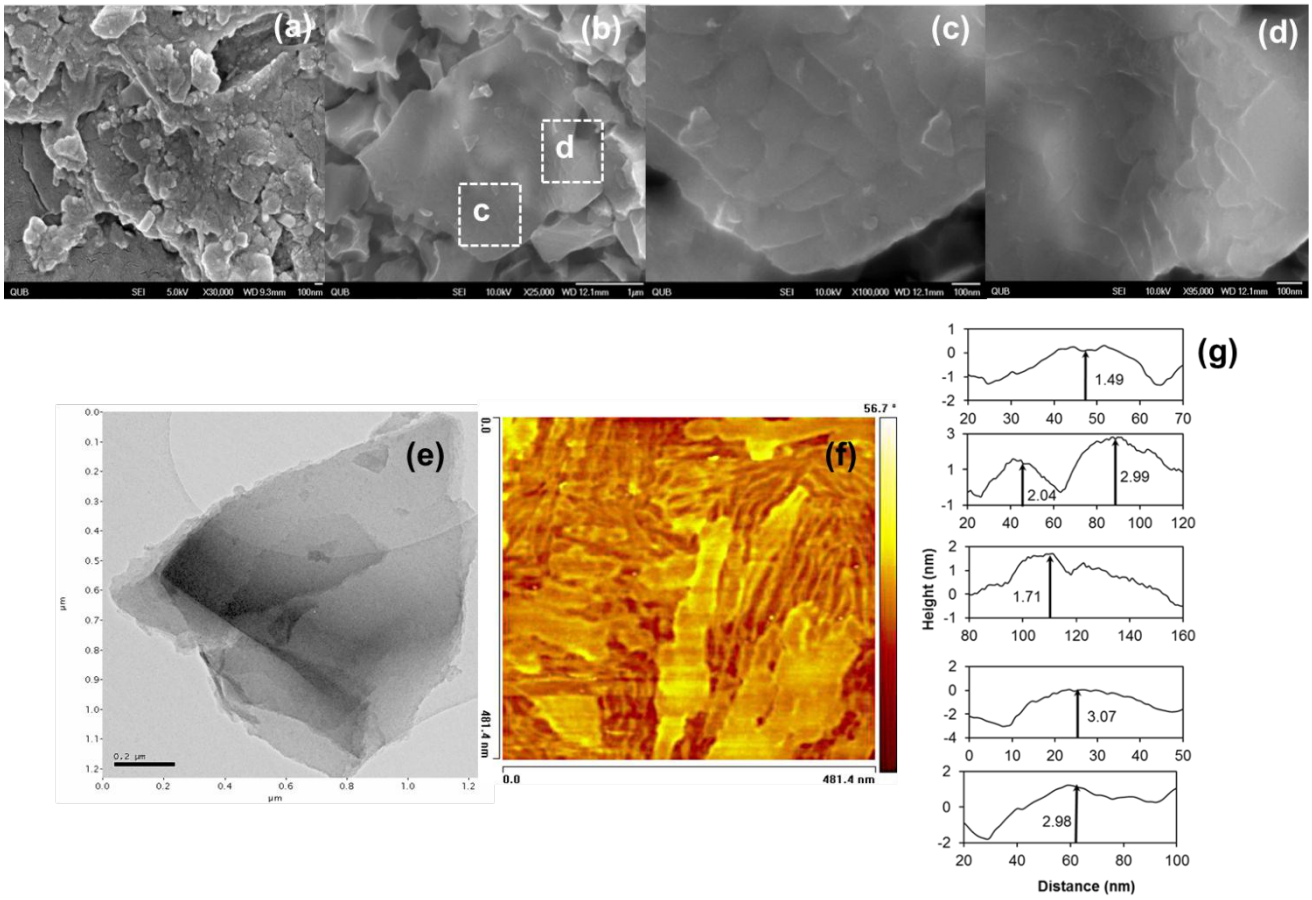

Figure 6. FESEM images of GO platelet structure after centrifugation at a) low and b)-d) high magnification, e) HRTEM image of GO showing individual GO layers in thin stack, f) tapping mode AFM phase image and g) associated feature height profiles at different positions.

The FESEM images (Figure 6(a-d)) show a GO platelet structure with relatively low surface roughness and curled edges and with no rod-like shaped structures detected, again suggesting the total removal of the sodium carbonate by-product. The TEM and AFM results (e-g) proved that the solvothermal process was able to produce very thin GO sheets (2-4nm thick) with lengths up to *ca* 1.3µm.

View Article Online
DOI: 10.1039/C9NR04202D

3.2 Characterization of composites of PCL and GO

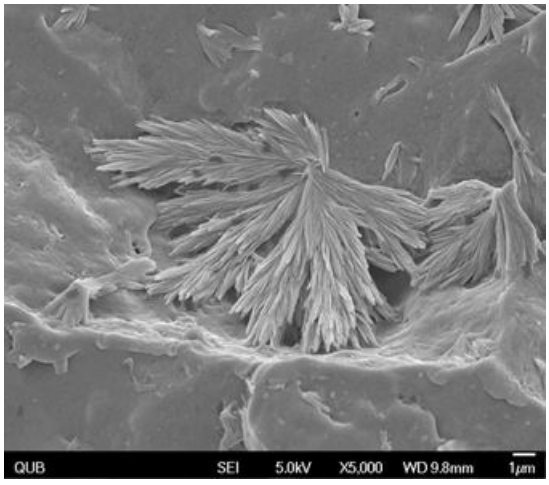

Figure 7: FESEM image of a "flower-like" structure of GO (3wt%) in PCL.

FESEM was used to study the morphology of the PCL/GO composite materials. Figure 7 shows an FESEM image of 3wt% GO in PCL indicating the presence of a flower-like shape associated with the interwoven rodlike crystals of the GO in the polymer matrix. Sun Hwa Lee *et al*. [32] have proposed that it is this wrinkled morphology that is the main cause of such flower-like shaped GO crystals. Shengua Lv *et al.*[33] reasoned that the content of GO in the PCL influences the formation of flower-shape crystals. In particular, they suggest that at low GO content, only a few "petals" are visible at the fracture surface which therefore produces "closed flowers", while at higher GO content, the petals start to get more dense thereby forming "opened flowers".

The effect of GO on the melting and crystallization behaviour of PCL was studied by DSC. The melting and cooling curves for various wt% of GO in PCL are shown in Figure 8(a) and (b), respectively. The associated thermal parameters determined from these and plots are listed in Table 1.

View Article Online
DOI: 10.1039/C9NR04202D

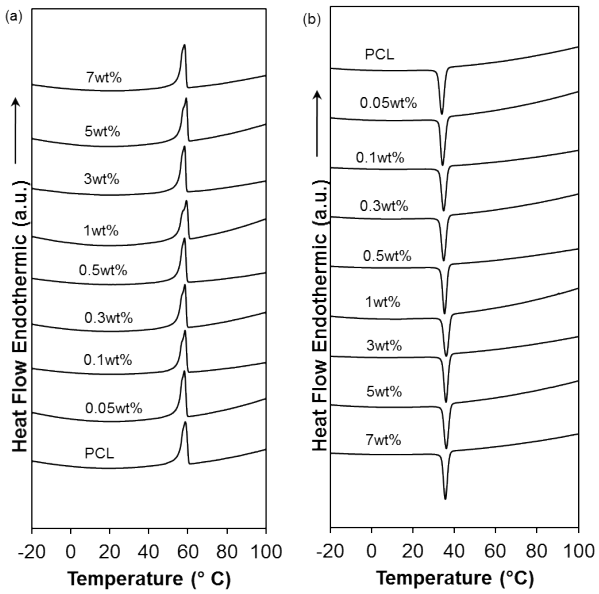

Figure 8. DSC thermograms of PCL and composites of PCL and GO at various wt% for second heating (a) and cooling (b) scans. (Samples were heated from -35 ^{o}C to 120 ^{o}C, held at 120 ^{o}C for 3 mins., then cooled to -35 ^{o}C, then held at -35^{o}C for 3 mins. And, subsequently heated to 120 ^{o}C at 10 ^{o}C/min.

Table 1. Thermal parameters for PCL and its composites with various wt% GO values. Crystallinity (X_c%) was calculated from $[\Delta H_m\ (1\text{-}x_f)/\Delta'H_m]x100$, where ΔH_m is the variation in the melting enthalpy of the composites obtained from DSC, $\Delta'H_m$ is the variation of melting enthalpy for a theoretical PCL crystal with infinite dimensions (135.44 J/g) and x_f is GO wt%[34].

GO wt%	T_m (^{o}C)	ΔH_m (J/g)	$FWHM_m$ (J/g)	T_c (^{o}C)	ΔH_c (J/g)	$FWHM_c$ (J/g)	X_c (%)
0	59	42	3	34	50	2	31
0.05	58	40	3	34	49	2	30
0.1	58	39	3	35	48	3	29
0.3	58	41	3	35	50	2	30
0.5	58	39	3	35	48	2	29

View Article Online
DOI: 10.1039/C9NR04202D

1	59	41	4	36	50	3	30
3	58	40	3	36	48	2	29
5	59	39	3	36	46	3	27
7	58	37	3	36	46	2	25

The addition of GO to PCL up to 7 wt% has no effect on T_m and only a modest effect on T_c (↑2°C), with the latter most probably within experiemental error. However, the enthalpy of fusion (ΔH_m) and crystallizzation (ΔH_c) both decreased with increased GO addition, although there was no change in crystallite size distribution observed from $FHWM_m$ and $FHWM_c$ which were both constant at 3 J/g and 2 J/g, respectively. X_c of PLC decreased from 31% to 25% on addition of 7wt% GO. Clearly, increasing addition of GO hinders PCL chain mobility and folding and thus crystallisation.

Additional XRD measurments were performed to study the effect of GO on the crystalline planes of PCL.

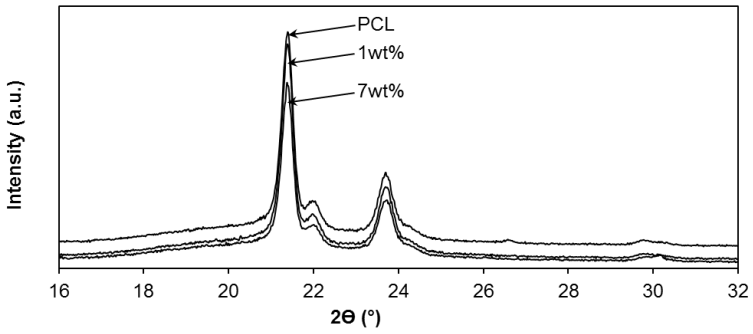

Figure 9. WAXD diffractogramms of PCL and its composites with GO at 1wt% and 7 wt% loading.

XRD scans for 1wt% and 7wt% GO in PCL are shown in Figure 11 with the pristine polymer provided for comparison and show major peaks at 2θ = 21.5°, 22.1°, and 23.8°

View Article Online
DOI: 10.1039/C9NR04202D

due to (110), (111), and (200) planes of PCL [35]. After incorporation of GO, the crystalline characteristics of the matrix are retained, as evident from the presence of the unchanged crystalline peaks, but a slight decrease in crystalline content is reflected by the decreased peak intensities, but this most likely to be withing instrument error.

The thermal stability of PCL and its composites with GO was studied by further TGA/DTGA analysis.

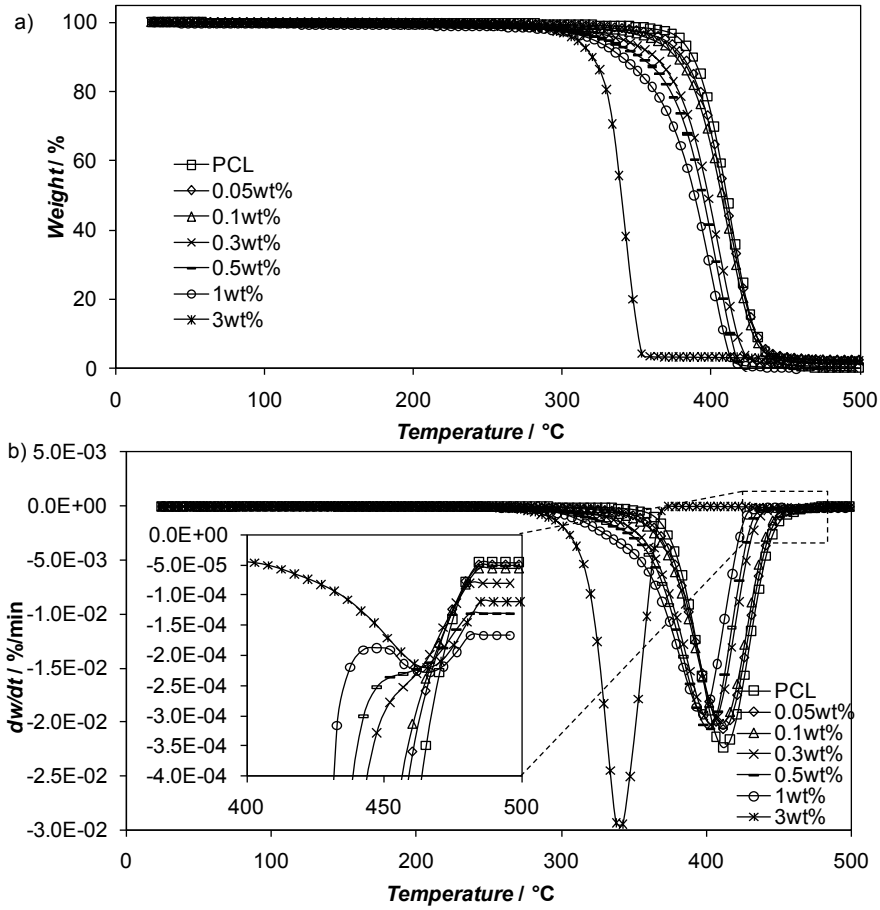

View Article Online
DOI: 10.1039/C9NR04202D

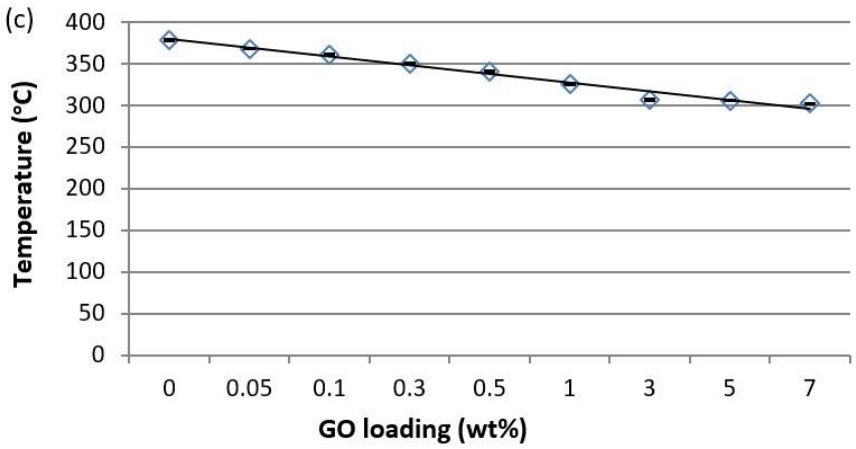

Figure 10: TGA (a) DTGA (b) of GO, PCL and composites of PCL at various wt% GO loading and c) change in the onset of degradtion temperature mass loss as a function of wt% GO content.

The addition of GO is seen to degrade the thermal stability of PCL as evident from Figure 10 (a) and (b), particulary when the GO content was greater than 1wt%. Figure 10(c) shows a reduction of the degradation point registered at 5wt% weight loss from 370^{o}C (neat PCL) to 300^{o}C (7wt% of GO).

The dynamical mechanical properties of the composites of PCL and GO were measured by DMA analysis.

View Article Online
DOI: 10.1039/C9NR04202D

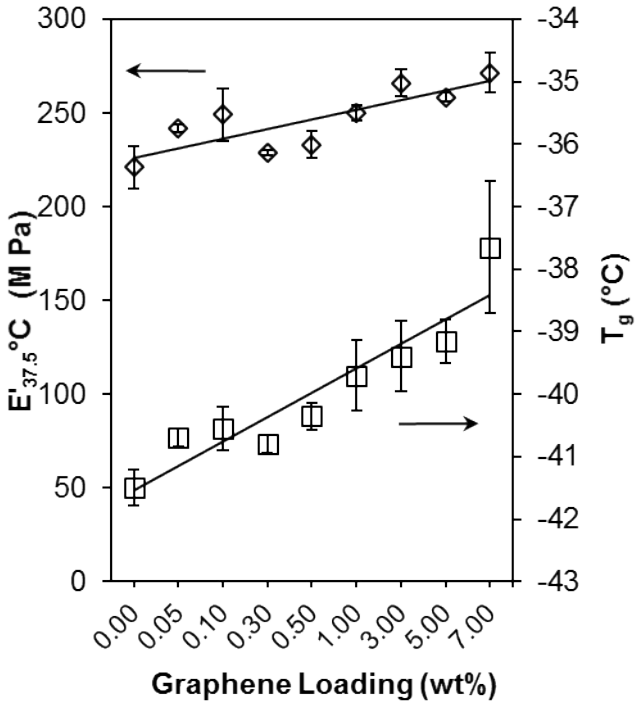

Figure 11. Variation in storage modulus at 37.5°C and T_g of PCL as function of GO loading.

As seen in Figure 11, addition of GO at various wt% loading results in an increase (11.5%) in the storage modulus, E‘ of PCL from 230 MPa to 260 MPa and an increase in the T_g of about 4 °C the from -41.5 °C to -37.5°C for the addition of 7wt% GO. The stiffening of PCL upon GO incorporation is associated with the formation of an interconnected GO network which hinders normal polymer chain dynamics. The 5.8% increase in E‘ from 230 MPa of neat PCL to *ca* 245 MPa achieved for a low GO content (0.05wt%) may be due to the particular flower-like morphology of GO crystals as seen in the FESEM study. Indeed, the interwoven rod-like crystals might facilitate an interconnection among filler particles, which causes the stiffening of the final composite even at small filler content [32, 33].

View Article Online
DOI: 10.1039/C9NR04202D

The electrical conductivity (σ) of the composites of the purified GO and PCL was determined from DC electrical resistivity measurements. PCL is an electrical insulator with about $\sigma=10^{-12}$ S/cm.

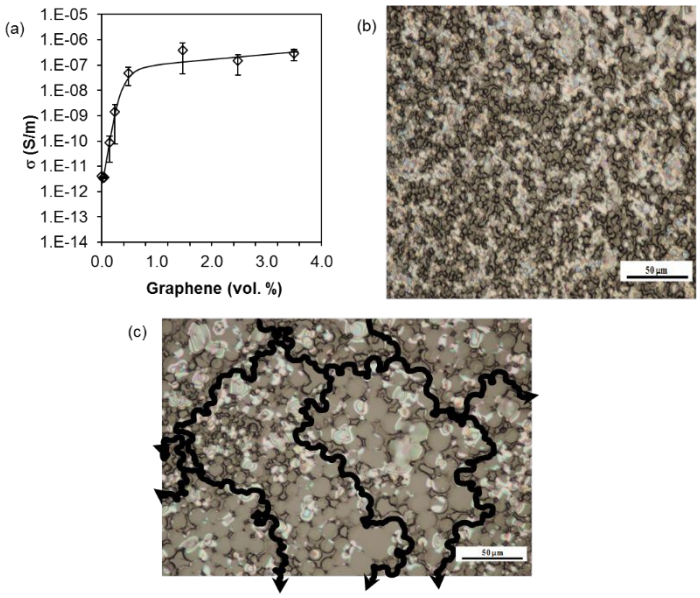

Figure 12. Change in DC electrical conductivity as a function of GO volume (%) (a). Optical micrographs showing GO is well distributed in the PCL matrix (b) and, when the PCL is partially molten where a continuous percolated GO network (black line) is observed (c).

As illustrated in Figure 12(a), addition of GO to PCL resulted in an increase in σ by about 5 orders of magnitude to 10^{-7} S/m for 1.5 vol% GO; a value in excess of that required for anti-static applications. Interestingly, an electrical percolation treshold was achieved for a GO loading as low as 0.5 vol%. Figure 12(b) shows an optical micrograph for PCL with 1 wt% GO in which the GO (dark regions) are seen to be well dispersed and evenly distributed in the PLC matrix. The interconnected GO network is more obvious when the

View Article Online
DOI: 10.1039/C9NR04202D

PCL is slowly melted, as seen in Figure 12(c), where the tracks of GO can be traced, as shown by the overlaid arrows.

4. Conclusions

GO was readily synthesized using a solvothermal process utilizing ethanol and sodium in a bomb calorimeter. A final purification step using centrifugation totally removed the sodium carbonate by-product formed during GO synthesis. The resulting GO contained no impurities and was added to PCL at loadings of up to 7wt% via extrusion without degrading. A summary of the characterization results for GO and composites of PCL and GO are presented in Table 2.

Table 2. Structure of GO and properties of composites of PCL and GO.

GO characterization		
Solvothermal process step	Technique	Results
1: precursor synthesis	Raman	No graphenic forms (no D, G bands)
2: 1st pyrolysis	Raman	GO formation (D band at 1350 cm^{-1} , G band 1580 cm^{-1})
3: washing	Raman	G band increase (higher crystalline quality)
	XPS	Reduction of oxidated sites and increase of C-C/C=C bonds (graphenic structure)
4: 2nd pyrolysis	FTIR	Reduction of OH/COOH, C-O bands; increase of C=C bands (graphenic structure)
	SEM/XRD	Sodium carbonate impurities
5:purification by centrifugation	TGA	Thermal stability enhanced compared to the un-purified product
	EDX	Sodium carbonate removal

View Article Online
DOI: 10.1039/C9NR04202D

SEM/TEM/AFM	GO platelets of nm thickness (*ca* 3nm) and μm length (up to *ca* 1.3μm)

Characterization of PCL composites with GO

Technique	Results
SEM	Flower-like structure of GO within PCL
DSC	No change in T_m, T_c, crystallinity and crystallites distribution of PCL
XRD	No change of PCL crystalline planes
DMA	Increase of E‘ (260MPa) and T_g (-38.5^{o}C) at 7wt% GO → stiffening
TGA	Improved PCL thermal stability upon GO incorporation ($T_{onset\ 5wt\%\ loss}$= 300^{o}C (7wt%GO))
EC	Electrical percolation at 0.5 vol%; σ_{max} at 1.5 vol% =10^{-7} S/m
OM	GO network formation within PCL matrix

Pyrolysis is an essential step in the synthesis of graphitic carbon materials post the first stage of the solvothermal process, with Raman spectra being able to distinguish between the precursor and pyrolized product (steps 1-2). Subsequent washing (step 3) resulted in the reduction of oxidized sites on the GO thereby increasing the graphenic structure (Raman, XPS) – sp^2 hybridization. A 2nd pyrolysis (step 4) further improved the graphenic structure of the GO, observed as a further reduction in the concentration of OH/COOH, C-O groups and a simultaenous increase of C=C bonding (FTIR), though impurities from the by-product (sodium carbonate) were still present (XRD). The final centrifugation step (step 5) resulted in the total removal of sodium carbonate (EDX) and the formation of thin GO (*ca* 3nm) platelets with lateral dimensions up to *ca* 1.3 μm (TEM, AFM).

Examination of composites of GO and PCL revealed ´flower-liké domains dispersed in the PCL matrix (SEM), derived from the wrinkled morphology of GO. No

View Article Online
DOI: 10.1039/C9NR04202D

change in PCL crystallinity and crystal structure was detected upon GO incorporation (DSC, XRD), though the dynamic modulus of PCL increased by about 10% (DMA). Purification and the increased graphenic nature of the GO resulted in an increase in electrical conductivity (↑10^5) and an electrical percolation threshold detected at low GO content (0.5vol%) (EC, OM).

The solvothermal synthesis and purification approach described in this paper provides a facile route for the preparation of a GO with a structure and properties useful as a functional filler for polymers.

Acknowledgements

The authors thank Dr Bronagh Millar, Dr Paula Douglas, Graham Garrett, John Kelso and Yian Wei Low for technical assistance. SJC thanks QUB for funding her studentship.

References

[1] Geim AK, Novoselov KS. The rise of graphene. Nat Mater. 2007;6:183-91.

[2] Park S, Ruoff RS. Chemical methods for the production of graphenes. Nat Nanotechnol. 2009;4:217-24.

[3] Zhu YW, Murali S, Cai WW, Li XS, Suk JW, Potts JR, et al. Graphene and Graphene Oxide: Synthesis, Properties, and Applications. Adv Mater. 2010;22:3906-24.

[4] Dreyer DR, Park S, Bielawski CW, Ruoff RS. The chemistry of graphene oxide. Chem Soc Rev. 2010;39:228-40.

View Article Online
DOI: 10.1039/C9NR04202D

[5] Compton OC, Nguyen ST. Graphene Oxide, Highly Reduced Graphene Oxide, and Graphene: Versatile Building Blocks for Carbon-Based Materials. Small. 2010;6:711-23.

[6] Choucair M, Thordarson P, Stride JA. Gram-scale production of graphene based on solvothermal synthesis and sonication. Nat Nanotechnol. 2009;4:30-3.

[7] Deng DH, Pan XL, Yu LA, Cui Y, Jiang YP, Qi J, et al. Toward N-Doped Graphene via Solvothermal Synthesis. Chem Mater. 2011;23:1188-93.

[8] Sun HM, Cao LY, Lu LH. Magnetite/reduced graphene oxide nanocomposites: One step solvothermal synthesis and use as a novel platform for removal of dye pollutants. Nano Research. 2011;4:550-62.

[9] Wu JL, Shen XP, Jiang L, Wang K, Chen KM. Solvothermal synthesis and characterization of sandwich-like graphene/ZnO nanocomposites. Appl Surf Sci. 2010;256:2826-30.

[10] Wang P, Jiang TF, Zhu CZ, Zhai YM, Wang DJ, Dong SJ. One-Step, Solvothermal Synthesis of Graphene-CdS and Graphene-ZnS Quantum Dot Nanocomposites and Their Interesting Photovoltaic Properties. Nano Research. 2010;3:794-9.

[11] Wang B, Park J, Su DW, Wang CY, Ahn H, Wang GX. Solvothermal synthesis of CoS2-graphene nanocomposite material for high-performance supercapacitors. J Mater Chem. 2012;22:15750-6.

[12] Zhang FY, Li YJ, Gu YE, Wang ZH, Wang CM. One-pot solvothermal synthesis of a Cu2O/Graphene nanocomposite and its application in an electrochemical sensor for dopamine. Microchim Acta. 2011;173:103-9.

View Article Online
DOI: 10.1039/C9NR04202D

[13] Nethravathi C, Rajamathi M. Chemically modified graphene sheets produced by the solvothermal reduction of colloidal dispersions of graphite oxide. Carbon. 2008;46:1994-8.

[14] Shah M, Zhang K, Park AR, Kim KS, Park NG, Park JH, et al. Single-step solvothermal synthesis of mesoporous Ag-TiO_2-reduced graphene oxide ternary composites with enhanced photocatalytic activity. Nanoscale. 2013;5:5093-101.

[15] Wang GX, Wang B, Park J, Yang J, Shen XP, Yao J. Synthesis of enhanced hydrophilic and hydrophobic graphene oxide nanosheets by a solvothermal method. Carbon. 2009;47:68-72.

[16] Dubin S, Gilje S, Wang K, Tung VC, Cha K, Hall AS, et al. A One-Step, Solvothermal Reduction Method for Producing Reduced Graphene Oxide Dispersions in Organic Solvents. ACS Nano. 2010;4:3845-52.

[17] Chen G. Phonon heat conduction in nanostructures. Int J Therm Sci. 2000;39:471-80.

[18] Mortazavi B, Ahzi S. Thermal conductivity and tensile response of defective graphene: A molecular dynamics study. Carbon. 2013;63:460-70.

[19] Hua L, Kai W, Inoue Y. Synthesis and characterization of poly(epsilon-caprolactone)-graphite oxide composites. J Appl Polym Sci. 2007;106:1880-4.

[20] Wan CY, Chen BQ. Poly(epsilon-caprolactone)/graphene oxide biocomposites: mechanical properties and bioactivity. Biomedical Materials. 2011;6.

[21] Hua L, Kai WH, Inoue Y. Crystallization Behavior of poly(epsilon-caprolactone)/graphite oxide composites. J Appl Polym Sci. 2007;106:4225-32.

View Article Online
DOI: 10.1039/C9NR04202D

[22] Kai WH, Hirota Y, Hua L, Inoue Y. Thermal and mechanical properties of a poly(epsilon-caprolactone)/graphite oxide composite. J Appl Polym Sci. 2008;107:1395-400.

[23] Cao YW, Feng JC, Wu PY. Preparation of organically dispersible graphene nanosheet powders through a lyophilization method and their poly(lactic acid) composites. Carbon. 2010;48:3834-9.

[24] Choi HJ, Kim JW, To KW. Electrorheological characteristics of semiconducting poly(aniline-co-o-ethoxyaniline) suspension. Polymer. 1999;40:2163-6.

[25] Dao TD, Oh KM, Choi JT, Lee HI, Jeong HM, Kim YS, et al. The Effect of Oxidation on Properties of Graphene and Its Polycaprolactone Nanocomposites. J Nanosci Nanotechnol. 2012;12:8420-30.

[26]http://antoine.frostburg.edu/chem/senese/101/inorganic/faq/carbonate-decomposition.shtml 06/07/2018

[27] Yang D, Velamakanni A, Bozoklu G, Park S, Stoller M, Piner RD, et al. Chemical analysis of graphene oxide films after heat and chemical treatments by X-ray photoelectron and Micro-Raman spectroscopy. Carbon. 2009;47:145-52.

[28] Kudin KN, Ozbas B, Schniepp HC, Prud'homme RK, Aksay IA, Car R. Raman spectra of graphite oxide and functionalized graphene sheets. Nano Lett. 2008;8:36-41.

[29] Tan PH, Deng YM, Zhao Q. Temperature-dependent Raman spectra and anomalous Raman phenomenon of highly oriented pyrolytic graphite. Phys Rev. 1998;58:5435-9.

[30] Bera M, Chandravati, Gupta P, Maji PK. Facile One-Pot Synthesis of Graphene Oxide by Sonication Assisted Mechanochemical Approach and Its Surface Chemistry. J Nanosci Nanotechnol. 2018;18:902-12.

View Article Online
DOI: 10.1039/C9NR04202D

[31] Wang HL, Hao QL, Yang XJ, Lu LD, Wang X. Graphene oxide doped polyaniline for supercapacitors. Electrochem Commun. 2009;11:1158-61.

[32] Lee SH, Kim HW, Hwang JO, Lee WJ, Kwon J, Bielawski CW, et al. Three-Dimensional Self-Assembly of Graphene Oxide Platelets into Mechanically Flexible Macroporous Carbon Films. Angew Chem Int Ed. 2010;49:10084-8.

[33] Lv SH, Ma YJ, Qiu CC, Sun T, Liu JJ, Zhou QF. Effect of graphene oxide nanosheets of microstructure and mechanical properties of cement composites. Constr Build Mater. 2013;49:121-7.

[34] Kweon H, Yoo MK, Park IK, Kim TH, Lee HC, Lee HS, et al. A novel degradable polycaprolactone networks for tissue engineering. Biomaterials. 2003;24:801-8.

[35] Chen JP, Chang YS. Preparation and characterization of composite nanofibers of polycaprolactone and nanohydroxyapatite for osteogenic differentiation of mesenchymal stem cells. Colloids Surf B Biointerfaces. 2011;86:169-75.